Cold Regions Science and Technology, 10 (1985) 141–151
Elsevier Science Publishers B.V., Amsterdam – Printed in The Netherlands

SNOW AVALANCHE FREQUENCY AND VELOCITY FOR THE KANANASKIS VALLEY IN THE CANADIAN ROCKIES

E.A. Johnson, L. Hogg and C.S. Carlson

Department of Biology and Kananaskis Centre for Environmental Research, University of Calgary, Calgary, Alberta (Canada)

(Received April 25, 1984; accepted in revised form September 4, 1984)

ABSTRACT

Avalanche frequency and predicted velocity are determined for a standardized runout distance for a large number of avalanche paths in the Kananaskis Valley, Alberta. The standardized runout distance is defined as the path segment with a 10-degree slope. Predicted velocities are calculated using the center-of-mass model of avalanche motion; frequencies are estimated using dendrochronological techniques. Results show velocities and average interval between avalanches to be positively correlated. Average slope angle of the entire avalanche path is a good indicator of both velocities and average interval. Paths with steeper average slope angle have longer average intervals between avalanches and larger expected velocities in the 10 degree slope runout position. Effects of avalanche frequency and velocities on changing vegetation cover from shrubs to trees is suggested to be due to differences in plant growth rates and life span.

INTRODUCTION

Frequency and velocity are two significant features of snow avalanches at specific slope locations. The objective of this study is to compare the expected frequency and velocities of snow avalanches in a standardized runout position on a large number of avalanche paths in the Kananaskis Valley, Alberta (Fig. 1). Avalanche frequency decreases from catchment to the extreme runout. This changing frequency requires that the slope position of a study be defined in order to make comparisons between avalanche paths. The standardized runout position in the study is the path segment with a 10-degree angle. This reference segment was chosen because, for the Kananaskis Valley, it is in the zone of intermediate (5–20 years) avalanche return interval. This is also the zone where slight increases in avalanche interval allow trees enough time to overtop the shrubby birches. Shrubby birches dominate the parts of the path with shorter avalanche intervals. Trees are always present as seedlings and saplings in this shrub vegetation, but are broken off or uprooted as soon as they reach the height of the shrub canopy. The trees are usually about 10 cm basal diameter at this point.

Historical records of avalanche velocity or runout distances do not exist for any of the paths studied. Consequently, we used the accepted approach of *predicting* the range of velocities by equations which model avalanche motion (Mears, 1981). The reader must note that these values are not empirical but predicted. Empirical values of velocity would certainly be different but, if the equations of motion capture the essential behaviour of avalanches, then the *patterns* of velocities should be realistic with the assumption given.

Most models of avalanche motion that are used in practice are of two types: those which view the avalanche as a fluid (Voellmy, 1955; Salm, 1966; Leaf and Martinelli, 1977; Buser and Frutiger, 1980), and those which view the avalanche as a moving center-of-mass (Kozid, 1962; Mellor, 1968; Perla et al., 1980; McClung and Schaerer, 1983). Voellmy's fluid model assumes that the avalanche is an endless fluid in a state of non-accelerating flow through Eulerian co-ordinates fixed to the channel (Voellmy,

0165-232X/85/$03.30

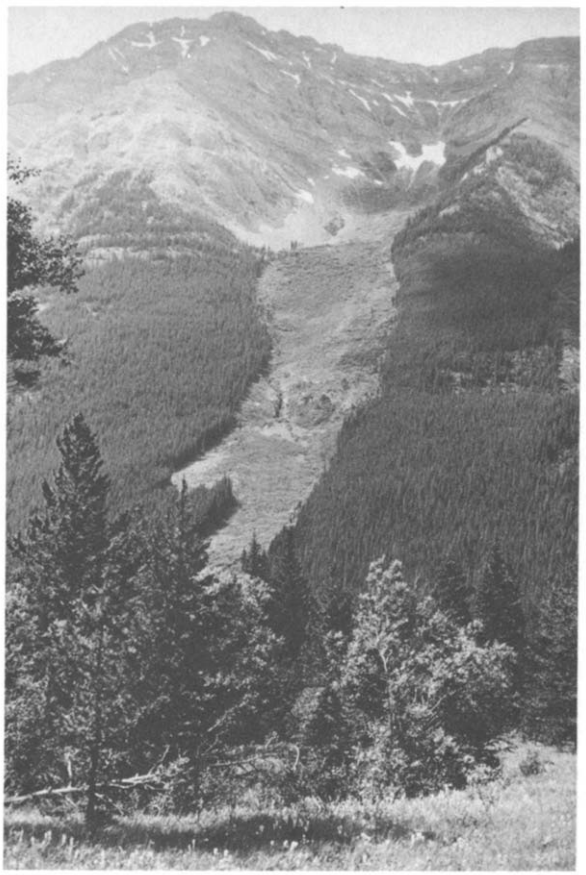

Fig. 1. View of snow avalanche path in Kananaskis Valley, Alberta.

1955). The unified center-of-mass model assumes that the avalanche is a mass enclosed by finite boundaries at any position at any time (Perla et al., 1980). The assumptions of both models are reviewed by Perla (1980). The endless-fluid and the center-of-mass models are essentially equivalent, provided one only seeks velocity and runout distance.

In both the endless-fluid and the center-of-mass models the solutions depend on: very analogous equations with a friction coefficient (μ) and dynamic resistance of either ξh (coefficient of turbulent friction and flow height) or M/D (avalanche mass/dynamic drag), depending on the model. Neither model has parameters which can be estimated precisely enough for one to have an obvious advantage. In this study we use the center-of-mass model; however, the substitution $\xi h/g$ for M/D can be made if one is more comfortable with an endless-fluid model.

Avalanche frequencies were estimated for the 10-degree slope segments from the ages of avalanche impact scars on trees and shrubs growing in the path. Because avalanches often occur at short intervals, great care was taken to ensure accurate dates between events recorded on the same plant and between plants. Missing or badly distorted rings are a common source of inaccuracies in assigning dates to particular rings. In order to minimize this error, undistorted ring-width series from a specimen were matched with a ring-width master chronology. A ring-width master chronology is the averaged standardized ring-widths from a large number of trees or shrubs from that site. All of the ring-widths in the master have been carefully verified to ensure accuracy of their dates (cf. Fritts, 1976). Besides accuracy in dating avalanche events, the event had to be replicated, *unambiguously* in several plants and a systematic search was made to discover all avalanche events. Avalanches may not leave records of their occurrence in every tree or shrub, but avalanches seem never to pass without some record being left. This was confirmed by comparison of tree and shrub records of avalanche events to a few paths with historical records. At present we do not know absolutely that the record is complete. Until the relationship of avalanches and the mechanics of scar formation are investigated, missed events must remain a possible source of error.

STUDY AREA

The 250 avalanche paths used in the Avalanche Velocity study and the subset of 21 in the Frequency study are situated on the upper reaches of the Kananaskis River in the Front Range of the Canadian Rockies. They are located in the Kananaskis Valley and extend from Galatea Creek (50°50′N) south to Elk Pass (50°35′N), and in the Smith–Dorrien Valley from Mud Lake (50°48′N) to the upper Kananaskis Lake (50°37′N). All snow avalanche paths in this area were first identified on aerial photos and then limited to those that could be confirmed in the field.

The paths are on the sides of the valleys of the Kananaskis river and three of its tributaries, the Smith–Dorrien, Boulton and Pocaterra creeks. These valleys run approximately NNW–SSE and occupy

weak Mesozoic clastic rocks. The ridges are sub-parallel thrust sheets and fault blocks which dip to the WSW and are of resistant Paleozoic carbonate rock. The valleys were glaciated during the Pleistocene and hence are U-shaped with relatively straight sides and no spurs. Intermittent streams issue into the main valley at more or less regular intervals from cirques and other high elevation areas of snow accumulation. The valleys tend to be slightly a-symmetric due to the tectonic structures. Because of the orientation of the ridges and valleys most of the avalanche paths have WSW or ENE aspects.

Located on the east side of the Rockies, the Kananaskis Valley and Smith–Dorrien Valley have dry climates. The average precipitation, over a 13-year period, at Kananaskis Lakes (elevation 1670 m) was: October to May, 360 mm; May to October, 250 mm (Eastern Rockies Forest Conservation Board, 1968). Precipitation varied throughout the valley, increasing about 20 mm for every 100 m of elevation gain. Heavy snowfalls do occur in the valley, usually in association with the movement of Arctic air masses from the north. The snow season lasts 8–10 months.

Foehn (chinook) winds occur, on average, about 30 times every winter (Longley, 1967). The winds have their greatest effect on the higher elevations in the valley because they flow over the dense cold air that settles in the valley bottoms. In the upper Kananaskis Valley the boundary between cold and warm air masses is approximately 1700 m. The high winds and elevated temperatures associated with foehns cause redistribution and melting of snow, which in turn affects snow stability on the avalanche paths.

The vegetation consists of a lower (1000–1400 m) montane zone of *Pinus contorta* var. *latifolia, Picea glauca* × *engelmanii* and an upper (1400–2100 m) subalpine zone of *Picea engelmanii, Pinus contorta* and *Abies lasiocarpa*. Tree line is at approximately 2100 to 2300 m. The catchment of most avalanche paths is at or above tree-line. The canopy vegetation of avalanche paths is predominately *Betula pumula* and *Salix* spp. with some saplings of *Picea* and *Abies* in the track and upper parts of the runout, and *Picea, Pinus* and some *Abies* in the runout (Fig. 1). Where the runout soil is fine-textured colluvium, *Populus tremuloides* may be common.

Avalanches usually begin to occur in December and can occur as late as early June. Dry snow avalanches occur in early and mid-winter (December to March) while wet and mixed snow avalanches can be expected in late winter and spring (March to June). Both loose-snow and slab avalanche types are present. Loose-snow avalanches usually extend only a short distance out of the catchment into the avalanche track, except on very steep slopes. Slab avalanches may come to rest in the track to the extremes of the runout.

Early and mid-winter snow packs often develop coarse granular snow and depth hoar near their bases because of shallow snow cover and cold temperatures. Avalanches often occur at these weak zones. Late-winter and spring snow packs are often stable because of settlement and compaction. They become unstable with the spring warming and melting.

AVALANCHE VELOCITIES

How far down a slope an avalanche will go depends on relatively unvarying forces such as gravity acting through the slope angle and vertical drop, and on variable forces such as the snow mass, bed roughness and ploughing. Thus, even when slope angle and vertical drop are constant, as they are on a particular path, the snow mass, bed roughness, and ploughing would appear for all two-parameter models of snow motion to produce a *variety* of velocities for the *same* stopping location. Direct measurements of velocity (e.g. Schaerer, 1973), although preferred, would have to be made over an inordinate number of avalanche events to establish this variation.

To estimate the range of velocities, we used the center-of-mass model of Perla et al. (1980) and the strategy of parameter computation of Bakkehoi et al. (1981) because we wanted a simulation which indicated the pattern of velocities possible under a range of avalanche conditions. Our objective was to evaluate the common factors which affect the range of velocities in a population of avalanche paths. Individual paths, besides the common factors, have particular factors which influence avalanche motion and require detailed, path-specific data. These detailed data on snow density, avalanche type, snow mass, path roughness, etc., are both impossible to obtain for past events and can only be subjectively

(observer-specific) determined when observable.

In the center-of-mass model, the tangential equation of motion on a path is:

$$Mv\,\mathrm{d}v/\mathrm{d}S = Mg\sin\theta - \mu \mathrm{Mg}\cos\theta - Dv^2 \qquad (1)$$

$$D = \mathrm{d}M/\mathrm{d}S + K$$

= driving force – friction – resistance

where M is the avalanche mass in kg, v is the velocity in ms^{-1}, S is the slope position in m, g is the acceleration of gravity in ms^{-2}, θ is the slope angle in degrees, μ is the coefficient of dynamic friction and K is the generalized ploughing and drag. Note that the resistive forces are proportional to v^2. μ, M/D and θ must be functions of S. M/D is also a function of the rate of entrainment. Further simplification gives the equation of motion for a center-of-mass:

$$\tfrac{1}{2}\,\mathrm{d}v^2/\mathrm{d}S = g(\sin\theta - \mu\cos\theta) - Dv^2/M \qquad (2)$$

The reader will find more detailed discussion of the models in Perla et al. (1980) and Bakkehoi et al. (1981).

Numerical computation

In order to calculate the avalanche velocities and runout distances for the center-of-mass model, the path is assumed to consist of several segments, each having constant slope. If segment (i) has length L_i, the moving center-of-mass velocity at the bottom of the segment is:

$$V_i^B = \sqrt{g(\sin\theta_i - \mu_i\cos\theta_i)(M/D)_i[1-\exp(-2L_i/(M/D)_i)] + (V_i^A)^2[\exp(-2L_i/(M/D)_i)]}\,. \qquad (3)$$

V_i^B is the solution of eqn. (2). Superscripts A and B indicate top and bottom of segment.

The velocity at the bottom and top of each segment may be calculated in this way, with the following correction for loss of momentum applied at the slope transition:

$$V_{i+1}^A = V_i^B\cos(\theta_i - \theta_{i+1})\,, \qquad (4)$$

where the slope is convex ($\theta_{i+1} > \theta_i$) no correction is made and $V_{i+1}^A = V_i^B$.

Equation (2) may also be solved for the runout distance in meters from the top of segment (i):

$$S = \frac{(M/D)_i}{2}\ln\left[1 - \frac{(V_i^A)^2}{g(\sin\theta_i - \mu_i\cos\theta_i)(M/D)_i}\right] \qquad (5)$$

Of course, the avalanche may not stop in segment (i) but may proceed into lower segments. Note that the parameters M/D and μ remain constant for all segments. This is unrealistic for actual avalanches but, since there exist no good data for how they vary along a path, the constant values are taken as the average M/D and μ for the whole path.

M/D and μ settings

In the equation given above, the path profile (in terms of L_i and θ_i) and the runout distance (in terms of the 10° segment) are defined for each path. The only values still to be defined are M/D and μ.

Our interest is not in predicting a specific velocity, given the path's profile and runout distance, but the realistic range of velocities that could be expected. This suggests that we need only define the pairs of M/D and μ which produce reasonable velocities. There is some empirical experience from a variety of sources as to these realistic ranges. Perla et al. (1980) summarize these as approximately:

$0.18 \leqslant \mu \leqslant 0.5$;

$10^2\ \mathrm{m} \leqslant M/D \leqslant 10^4\ \mathrm{m}$;

$10\ \mathrm{m/s} \leqslant v \leqslant 60\ \mathrm{m/s}$.

The procedure for calculating the range of μ, M/D values for specified slope profiles and runout position of 10° is to set the M/D value and then find a μ value for which the avalanche stops in the 10° segment. The algorithm for this is adapted from Bakkehoi et al. (1981). After assigning the M/D value the initial $\mu(1)$ is:

$$\mu(1) = 0.5\,(\mathrm{Max}_\mu + \mathrm{Min}_\mu) \qquad (6)$$

where Max_μ = tan (angle of top-most segment) and $\mathrm{Min}_\mu = 0$. The entrance and exit velocities of all path segments are computed from eqn. (3) and the runout distance from eqn. (5). If the avalanche stops above the 10° segment, substitute $\mathrm{Max}_\mu = \mu(1)$ and repeat the calculation. If the avalanche passes through the

TABLE 1

Example of results of avalanche simulation using Perla et al. (1980) center-of-mass model. Path E 3-22, vertical drop 546 m

Segments	Angle (°)	Length (m)	Velocity ($m\ s^{-1}$)							
			μ = 0.483, M/D 54600		μ = 0.468, M/D 5460		μ = 0.326, M/D = 546		μ = 0.177, M/D = 54	
			Upper	Lower	Upper	Lower	Upper	Lower	Upper	Lower
1	26.9	336	0	11.87	0	14.78	0	24.72	0	12.49
2	45.4	214	11.87	41.20	14.78	41.82	24.72	41.02	12.49	17.64
3	22.1	243	37.84	32.87	38.41	33.00	37.67	28.55	16.20	10.61
4	39.1	48	32.87	36.31	33.00	36.33	28.55	31.77	10.61	15.36
5	24.6	220	35.16	33.57	35.17	33.22	30.76	27.86	14.88	11.63
6	10.0	178	32.49	0	32.15	0	26.96	0	11.26	0

10° segment, substitute $\mathrm{Min}_{\mu} = \mu(1)$ and repeat. Values of μ were allowed to converge to three significant figures.

The settings of the M/D were $100Y$, $10Y$, Y and $Y/10$ where Y is the total vertical drop to the 10° path position. This is an allometric approach, suggested by Bakkehoi et al. (1981), where Y is used as a simple slope scale predictor. Instead of using Y, other strategies were tried using, for example, the cube root of the area of the catchment, the path length, and various subjective indices of path shape. With the exception of path length, all approaches involved substantial subjective judgement and the resulting patterns in velocity did not differ from those given by using Y.

Table 1 gives an example of the results of a simulation for one path.

Path measurements

250 avalanche path profiles were identified and mapped from aerial photographs on to a 1:50,000 topographic map. Path lengths were measured starting at approximately the center of the catchment. Each path was divided into segments of similar inclination. Horizontal map distance (HD) and vertical drop (VD) were measured within each segment on the map, and the length of the segment was calculated as:

$$L_i = (VD^2 + HD^2)^{1/2} . \tag{7}$$

The angle of inclination was determined by:

$$\theta_i = \arctan (VD/HD) . \tag{8}$$

"Average path angle" is the sum of the segment inclination multiplied by its length, all divided by the total path length:

$$\frac{\sum_{i=1}^{n} (L_i \theta_i)}{\sum_{i=1}^{n} L_i} . \tag{9}$$

Results

As was pointed out above, one of the properties of a two-parameter model of avalanche motion is that a large number of combinations of the two parameters (μ and M/D) will satisfy eqn. (3) for a given path's runout (Perla et al., 1980). This means that a graph of the μ and M/D values for a *specific* runout will not be a single point but a curve (Fig. 2).

Three characteristics are common to parameter curves of all 250 paths for runouts of 10 degrees: (1) a convergence of curves at $M/D = Y/10$ and μ = 0.18, (2) nearly constant μ values when M/D is very large, and (3) a difference in the slopes of the parameter curves between these two extremes.

The first characteristic describes avalanches in which the drag dominates the M/D ratio and μ is equal to tan 10°, the slope angle of the last segment. Since the drag dominates the equation of motion, the friction need have its effect only in the segment in which the avalanche is to stop. Therefore, only in the

10° segment are the slope driving forces (mg sin 10°) and the slope normal forces ($\mu\, mg$ cos 10°) balanced, allowing the avalanche to stop. The velocity on simple (monotonic) decreasing slopes is low and relatively constant until the last path segment. Friction values less than tan 10° for the final segment make little physical sense and hence explain the convergence of all path parameter curves at this value.

The second characteristic of the parameter curves describes avalanches in which the mass dominates the M/D ratio. In order for the avalanche to stop in the 10° segment, μ approaches the tangent of the angle of the top segment. The slope normal forces are therefore applied to the avalanche throughout the path. The velocity on simple (monotonic) decreasing slopes will peak near the top of the path and decrease towards the 10° segment. The segment in which the largest velocity occurs, in simple slopes, indicates the length of the path over which friction must be applied to stop the avalanche at the 10° segment.

At large M/D, the increase in M/D is not paralleled by an increase in μ, as shown in Fig. 2. The reason is found in the equation of motion. The friction must counter v^2 to stop the avalanche when the mass is very large and M/D is very small. Therefore, the μ values are related to v^2, as can be seen in Fig. 3.

The third characteristic of the parameter curves is the most useful for separating dynamically different paths. Between $M/D = Y/10$ and $M/D = 10/Y$ the μ

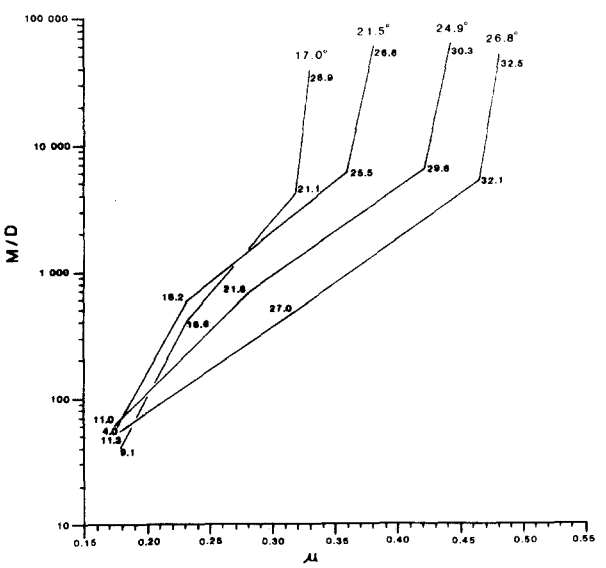

Fig. 2. Values of the coefficient of dynamic friction (μ) and mass to drag ratio (M/D) that give zero velocity (ms^{-1}) at the end of the 10° segment for avalanche paths having average slope angles of 17.0°, 21.5°, 24.9°, and 26.8°. Numbers next to the lines are the calculated velocities at the start of the 10° path segment with those parameter combinations.

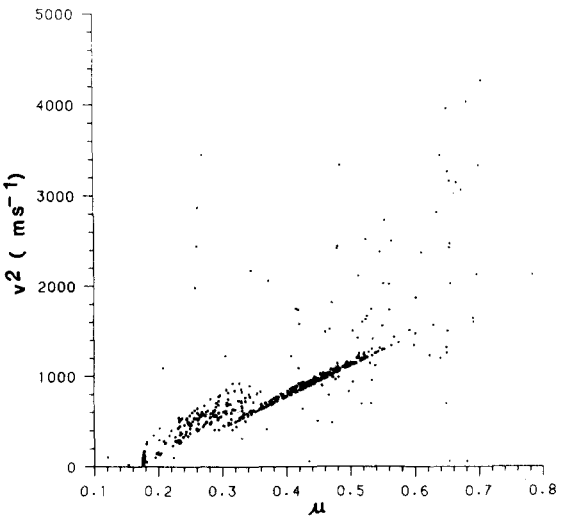

Fig. 3. The relationship of the dynamic friction coefficient (μ) to the velocity (v^2) at the beginning of each slope segment on all paths.

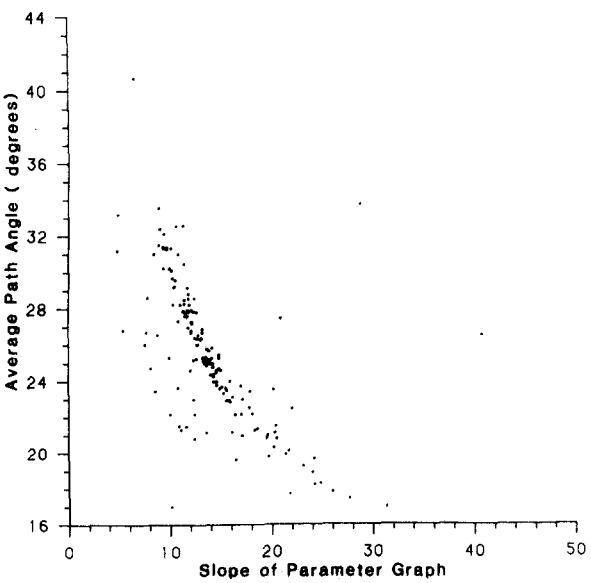

Fig. 4. The slope of the middle part of the curves of parameter values in Fig. 2 versus the average slope angle.

values increase at different rates for different paths. This produces the most obvious differences between parameter curves. These different rates are shown in Fig. 4 to be primarily related to the average steepness of the paths. On steep slopes, therefore, a higher μ is required at the same M/D to stop an avalanche in the 10° segment.

AVALANCHE FREQUENCY

An understanding of avalanches requires not only a study of the forces of motion but also of how often avalanches can be expected. We have already seen how, for the 10° runout position, the variation in velocities of avalanches can be simulated. Further, we have seen that the average slope angle for an avalanche path is the simplest indicator of the pattern of these velocities. Our objective now is to estimate the average number of years between avalanches (inverse of the avalanche frequency) which over-run the 10° segment.

Methods

The average interval between avalanches was estimated for the 10° segment on twenty-one paths using dendrochronological methods (Fritts, 1976). The use of annual growth rings means that only one avalanche each year can be identified. Paths were chosen so as to cover the range of average slope angles used in the velocity simulation.

Evidence of avalanches as recorded in the trees and shrubs was classified as impact damage and indirect effects. Impact damages were: impact scars on the avalanche-facing side of the stem, breakage of branches or terminal leaders followed by regrowth from adjacent branches or dormant buds, reaction wood caused by non-elastic bending, and, in some cases, stems broken or uprooted by the avalanche. This latter case is more difficult since it necessitates crossdating (Stokes and Smiley, 1968) the dead tree's ring-widths with living tree ring-widths. Indirect effects were: growth release in trees or shrubs caused by removal of adjacent over-story plants and recruitment of trees or shrubs after the avalanches. Evidence had to be unambiguously related to avalanches. All of the evidence mentioned *commonly* results from other causes, so temperance was always exercised in accepting evidence. Impact scars were used in almost all cases to establish the chronology. Reaction wood was so difficult to interpret that it was only rarely used (see Shroder, 1977).

Wedges or disks were taken from the trees and shrubs to date events. This was found to be the only means by which missing or badly contorted growth rings could be detected. Missing rings were very common in injured, slow growing and older trees. If searches for missing rings had not been made the resulting dates of avalanches would often have been in error by several years. Contorted rings near scars often produced different counts for different sides of the scar, even when great care was exercised. This is one of the reasons why disks and not wedges were preferred. Counts of growth rings alone rarely gave accurate dates of avalanches.

Each wedge or disk was carefully sanded so that a clear surface could be examined under the microscope. Two radii which were not seriously distorted by scars, reaction wood, etc., had their rings counted and marked with pin pricks at decade intervals. On disks these decade marks were traced to see if they matched. This was not usually possible in wedges. For both wedge and disk, ring-widths were measured to the nearest 0.1 mm. These ring-width series were then compared to master ring-width indices (cross-dating). These masters consist of ring-width series from 15 to 25 trees which have been standardized by having their growth and site specific trends removed (cf. Fritts, 1976). From these comparisons, ring-width patterns of particular narrow and/or wide rings identified certain marker years. These distinctive years could then be located on the wedge or disk and precise dating facilitated even when rings were missing or badly contorted.

For each 10° segment a large number of trees and shrubs (>15) were located and sampled in order to replicate the event record. A single plant, even if it is old, rarely records all the avalanches in its slope segment. All avalanches seem to leave evidence on some of the trees and shrubs. A large sample and careful searches minimize the possibility of missing avalanche events.

The individual tree event records were then compared using Cole's (1949, 1957 – as modified by Hurlbert, 1969) similarity index. The similarity index

allows the tree event records to be ordered from the most to the least similar records. The least similar records were then re-examined for errors in dating of events and possible events. A final synthesis of avalanche events was then created from the individual tree event records and this master event chronology used to determine the interval between avalanches. Shroder (1977) constructs a similar event plot, but uses it to confirm the co-occurrence of events in different trees without first confirming the accuracy of the *date* of the runs by cross-dating (Madany et al., 1982).

The number of intervals is always small, rarely greater than 10, but never less than 5. The length of the record varied from 40 to 80 years, depending on the path. Studies of avalanche chronologies for all path segments have shown that the shape of the distribution of avalanche intervals for a segment becomes increasingly symmetrical (Gaussian) as one moves down a path (Johnson, 1983). Therefore, taking an average of the intervals at the 10° segment seems to give a good approximation of the central tendency of the interval distribution. The standard error of the mean increases rapidly with average intervals larger than approximately 13 years. This is due to fewer events being recorded.

Results

Figure 5 gives the relationship of the estimated average avalanche interval ($\bar{T}$) of the 10° segment to the average path angle. The graph indicates that steep slopes (steep average path angle) have longer intervals between avalanches at the 10° segment. This suggests that on steep slopes avalanches do not run as far or as often. The result is that many avalanches only extend a short distance down the path and only rarely reach the 10° segment. On moderate slopes avalanches extend further down the path. Consequently, the 10° segment is reached more often. This pattern is supported by other studies of the chronologies of entire avalanche paths in the Kananaskis Valley (Johnson, 1983).

The velocities from the simulation for the entrance into the 10° segment also change systematically with the average interval between avalanches (Fig. 6). Steeper slopes have longer intervals between avalanches and produce potentially faster avalanches.

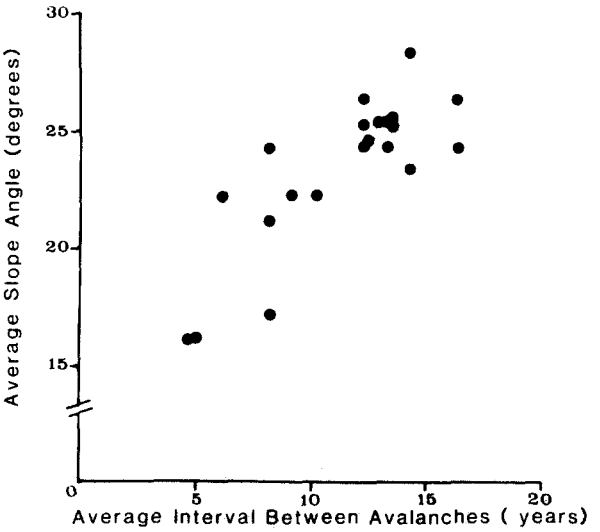

Fig. 5. Relationship of the estimated average avalanche interval ($\bar{T}$) of the 10° segment to the average slope angle for twenty-one avalanche paths.

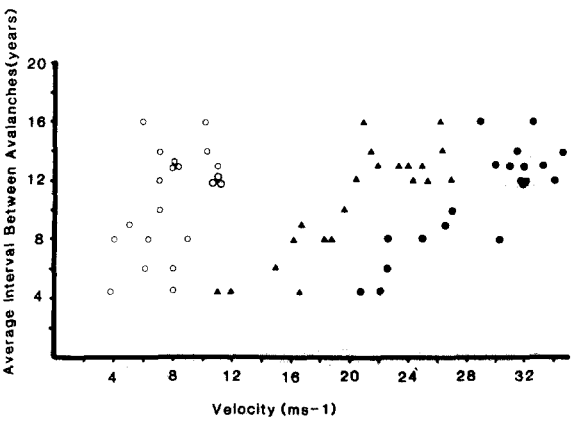

Fig. 6. Relationship of average return time ($\bar{T}$) versus the avalanche velocity from the simulation of motion for the 10° segment of 21 avalanche paths. ○ is for "wet" avalanches, i.e. $Y/10$, ▲ and ● are "dry" avalanches, i.e. Y, $10Y$ respectively.

Moderate slopes have shorter intervals between avalanches and produce potentially slower avalanches. Notice that, besides the range of velocities, the absolute velocities become smaller when drag dominates the ratio M/D.

Using the estimated average interval between avalanches ($\bar{T}$), it is possible to calculate the probability of an avalanche not occurring for a length of time N

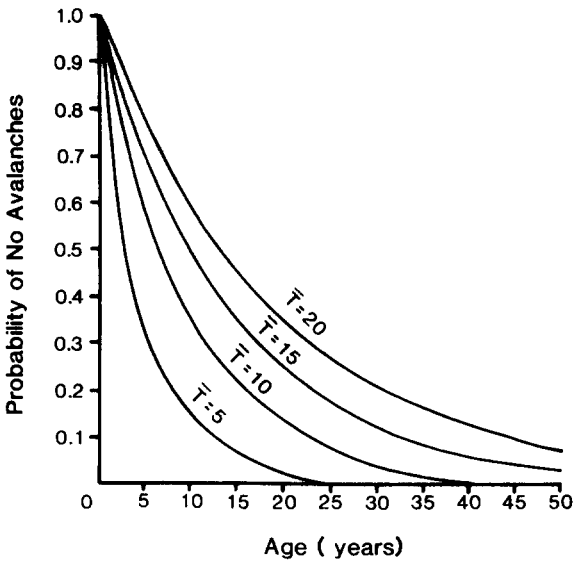

Fig. 7. Probability distribution of an avalanche not occurring for different average intervals between avalanches $\bar{T}$.

by using $P(N) = (1 - 1/\bar{T})^N$. $P(N)$ is a decreasing function of N at a rate determined by $\bar{T}$. Figure 7 shows these curves for the range of intervals between avalanches ($\bar{T}$), found in Fig. 5.

LIMITATIONS OF RESULTS

Avalanche frequency and velocities for the 10° slope position are *not* determined with the precision, manner and validity that would be preferred. Several limitations in the empirical data and in our understanding of avalanche processes are discussed below and must be kept firmly in mind when interpreting results.

Evaluation of avalanche hazards is strongest when the frequency of events of known velocities can be determined. In this study, frequency and velocity values are not connected. Instead we have two sets of information for a slope location: the event frequency and the expected range of velocities.

In theory it is possible to date avalanche events with scars and then determine the velocity of the event by the size range of trees broken. Mears (1975) has suggested how to determine the velocity of wet avalanches from the breaking stress of large-diameter trees for which the bole drag coefficient was 1. In practice, most slope positions do not offer a large enough range of tree diameters to bracket the avalanche velocity. Also, when smaller-diameter trees are used, the breakage model must take into account shear forces and the effect on drag and avalanche pressure distribution of the deflection of the tree before breakage.

Avalanche velocities have not been directly measured on a path. As was pointed out in the results, it is hard to see how direct measurements of velocities will ever be possible for any but a very few paths. Thus, indirect approaches which estimate velocity from knowledge of avalanche forces, appropriate variables and parameters of the path will always be necessary. However, our present knowledge of avalanche dynamics is primitive and all models are *simple* working hypotheses.

EFFECT OF FREQUENCY AND VELOCITIES ON TREES AND SHRUBS

Figure 6 showed a positive correlation between avalanche velocities (V) and the average interval between avalanches ($\bar{T}$). This suggests that in changing from a moderate to a steep slope, avalanches which reach the 10° segment should occur at longer intervals and be accompanied by an increase in velocities. These results would only be observed if: (1) the avalanches were stratified by similar M/D ratios as they are in Figure 6, (2) slope steepness were not consistently related to certain M/D ratios, and (3) path specific factors did not obscure the common factors.

With these restrictions in mind, there is the possibility that trees growing on paths of low avalanche frequency have a greater chance of living longer and thus of growing to a larger diameter before an avalanche. However, when the avalanche does occur its impact pressure will be greater and still cause the trees to be broken. This point makes clear that a more complete understanding of avalanche hazard requires that characteristics of the structure at risk be incorporated. Since trees and shrubs are normally found on avalanche paths, they are the logical first structures to be considered.

The effect of avalanches on trees and shrubs is a

complex problem (Mears, 1975; Johnson, 1983), but some interesting results can be obtained by a rather simple analysis. Figure 8 plots the mean diameter a tree or shrub would have reached at different average intervals between avalanches ($\bar{T}$). The diameters are for plants growing on the 21 paths used in the avalanche frequency determination. The standard error bars indicate variation in diameter due to differences in physical environments. Both pine and spruce have linear diameter growth over their first 30 years, while birch begin to slow down in diameter growth at about 15 years. The inherent life span of birch is short. Of over two hundred birches aged, only 6 were older than 18 years. Pine and spruce can live to over 200 years.

Birches appear to be favored in the 10° segment of moderately steep paths with short average intervals between avalanches. As a working hypothesis we suggest this is due to their smaller size and greater flexibility. Pine and spruce appear to be increasingly favored in the 10° segment on steep paths with longer average intervals between avalanches. This appears to be due to longer intervals between avalanches and allows them to overtop and shade the smaller birches. If avalanches do not occur for 20 years or longer, the combination of shade and short life span will eventually eliminate the birch.

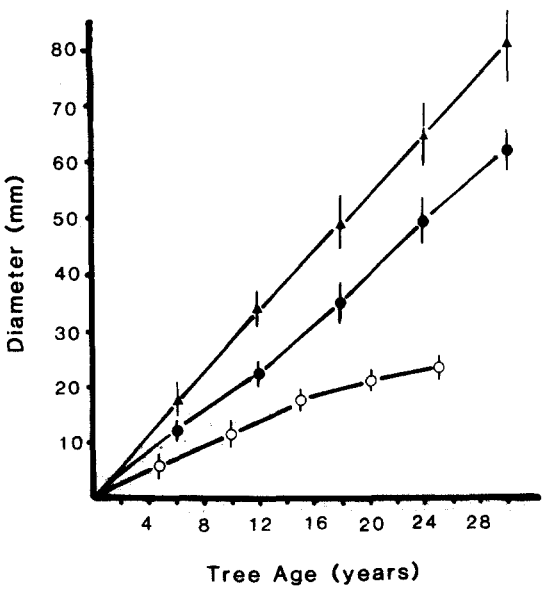

Fig. 8. Diameter growth of two trees (▲ Engelmann spruce [*Picea engelmanii* Parry ex Englm] and • Lodgepole pine [*Pinus contorta* Loudon]) and a shrub (○ Dwarf birch [*Betula pumila* L]) which dominate the vegetation on the lower part of avalanche paths in the Kananaskis Valley. Bars are standard errors of the mean.

ACKNOWLEDGMENTS

This study was supported by a grant from the Natural Sciences and Engineering Research Council of Canada to E.A. Johnson. Ron Perla and one anonymous referee gave substantial help to us. The personnel of Kananaskis Provincial Park – J. Murphy, R. Chamney, G. More and R. Gee – were always willing to help in our field work. J. Lancaster helped with the field work.

REFERENCES

Bakkehoi, S. Cheng, T., Domaas, U., Lied, K., Perla, R., and Schieldrop, B. (1981). On the computation of parameters that model snow avalanche motion. Can. Geotech. J., 18: 121–130.

Buser, O., and Frutiger, H. (1980). On observed maximum runout distance of snow avalanches and the determination of the friction coefficients μ and ξ. J. Glaciol., 26: 121–130.

Cole, L.C. (1949). The measurement of interspecific association. Ecology, 30: 411–424.

Cole, L.C. (1957). The measurement of partial interspecific association. Ecology, 38: 226–233.

Fritts, H.C. (1976). Tree Rings and Climate. Academic Press, New York.

Hurlbert, S.H. (1969). A coefficient of interspecific association. Ecology, 50: 1–9.

Johnson, E.A. (1983). A method for estimating the probability of avalanche induced bending and breakage in woody plants. Bull. Ecol. Soc. Amer., 64: 148.

Kozid, S.M. (1962). Raschet Dvizheniia Snezhnykh Lavin. Gidrometeoizdat, Leningrad, 76 pp.

Leaf, C.F., and Martinelli, M., Jr. (1977). Avalanche Dynamics: Engineering Applications for Land Use Planning. U.S. Dept. of Agriculture, Forest Service, Research Paper RM-183.

Longley, R.W. (1967). The frequency of winter chinooks in Alberta. Atmosphere, 5: 4–16.

Madany, M.H., Swetnam, T.W., and West, N.E. (1982). Comparison of two approaches for determining fire dates from tree scars. For. Sci., 28: 856–861.

McClung, D.M. and Schaerer, P.A. (1983). Determination of avalanche dynamic friction coefficient from measured speeds. Ann. Glaciol., 4: 170–173.

Mears, A.I. (1975). Dynamics of dense-snow avalanches interpreted from broken trees. Geology, 3: 521–523.

Mears, A.I. (1981). Design Criteria for Avalanche Control Structures in the Runout Zone. U.S. Dept. Agriculture, Forest Service, General Technical Report RM-84.

Mellor, M. (1968). Avalanches. Cold Regions Science and Engineering. Part III-A3d, 215 pp. U.S. Army, Corps of Engineers, Cold Regions Research and Engineering Laboratory, Hanover, NH.

Perla, R.I. (1980). Avalanche release, motion and impact. In: Colbeck, S.C. (Ed.), Dynamics of snow and ice masses. New York, Academic Press, pp. 397–462.

Perla, R., Cheng, T.T., and McClung, D.M. (1980). A two-parameter model of snow-avalanche motion. J. Glaciol., 26: 197–207.

Salm, B. (1966). Contribution to avalanche dynamics. In: Symposium international sur les aspects scientifiques des avalanches de neige, 5–10 Avril 1965, Davos, Suisse, p. 199–214. (Publication No. 69 de l'Association Internationale d'Hydrologie Scientifique).

Schaerer, P.A. (1973). Observations of Avalanche Impact Pressure. U.S. Dept. of Agriculture, Forest Service, General Technical Report RM-3, pp. 51–54.

Shroder, J.F., Jr. (1977). Dendrogeomorphological analysis of mass movement on Table Cliffs Plateau, Utah. Quat. Res. (N.Y.), 9: 168–185.

Stokes, M.A., and Smiley, T.L. (1968). An Introduction to Tree-Ring Dating. University of Chicago Press, Chicago.

Voellmy, A. (1955). Über die Zerstörungskraft von Lawinen. Schweizerische Bauzeitung, Jahrg. 73 (12): 159–162; (15): 212–217; (17): 246–249; (19): 280–285.